

Supplemental Information

Fig S1 The neonatal heart of NOD/SCID fails to regenerate. (A) Schematic diagram showing the experimental design. (B) Images of scar tissues at 4 weeks post CI to P3 or P8 hearts, scale bars: 2000 μm . (C, E, G) Masson's trichrome staining showing representative serial cross sections of fibrotic tissues in blue at 4 weeks post CI, scale bars: 1000 μm . (D, F, H) Quantification of fibrotic tissue coverage based on (C, E, G respectively). Data are presented as mean \pm S.E.M., n=6, *P<0.05, **P<0.01.

Figure S1

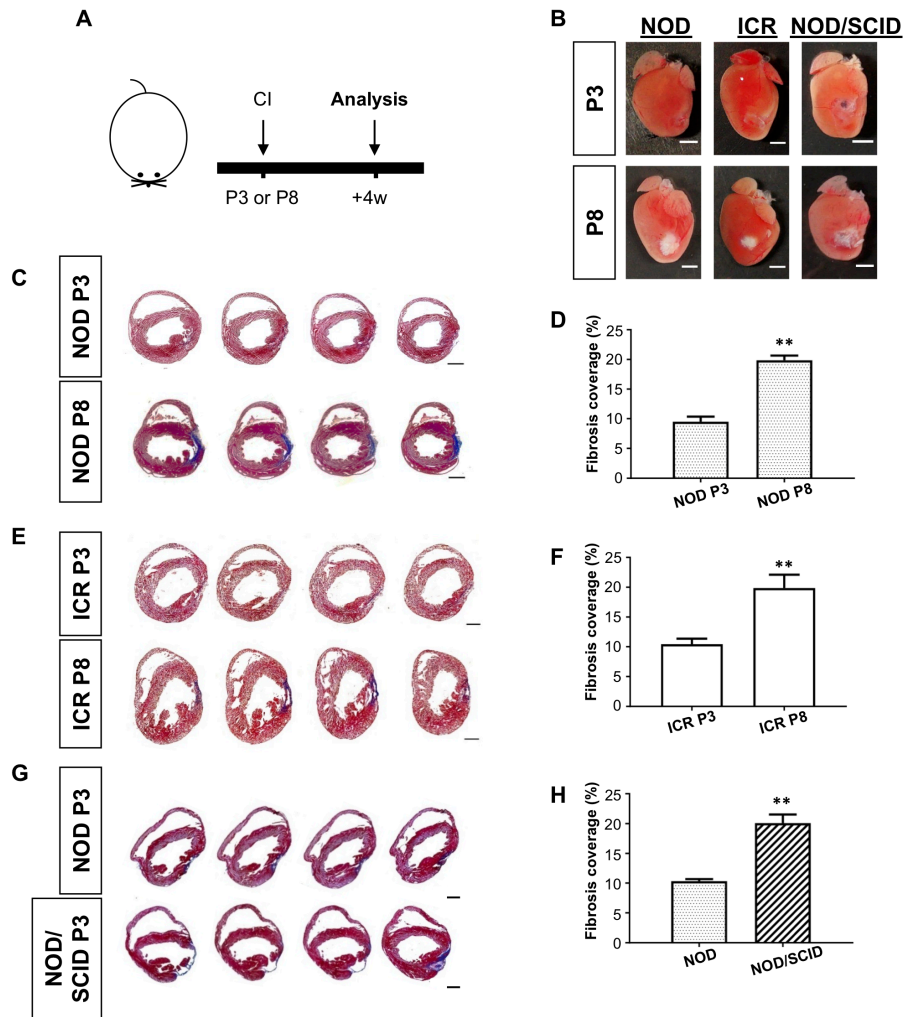


Fig S2 Echocardiography showing functional and morphological change during neonatal heart regeneration. (A, G) Schematic diagrams showing the experimental design. (B, H) Echocardiographic analyses and quantification showing (C, I) %fractional shortening; (D, J) %ejection fraction; (E, K) end-diastolic diameter (LVID d) or (F, L) end-systolic diameter (LVID s) at (A-F) 4 days or (G-L) 4 weeks post CI, n=6. (C-F, I-L). Data are presented as mean±S.E.M., *P<0.05, **P<0.01, ***P<0.001.

Figure S2

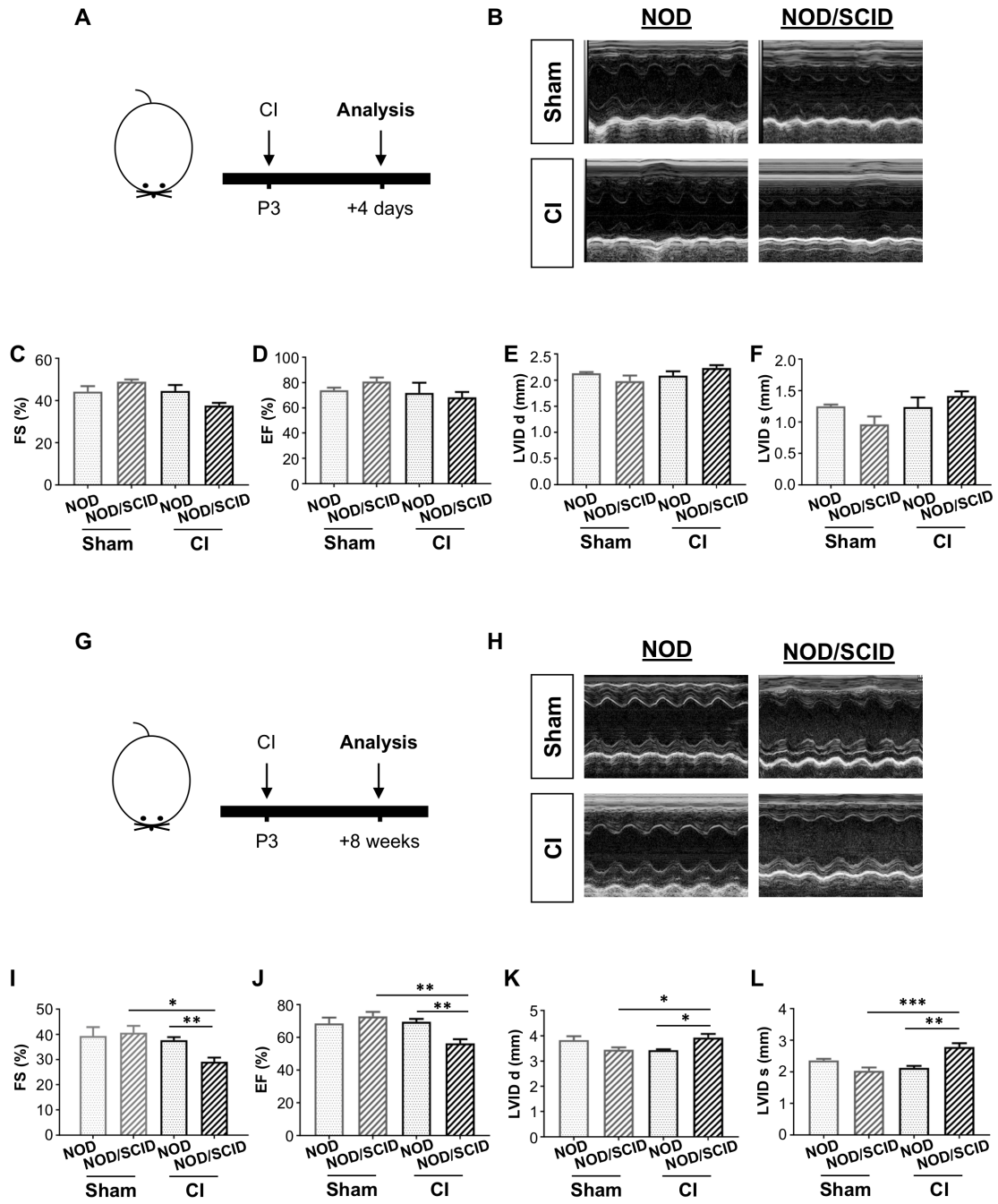


Figure S3 Quantification of Treg in the neonatal mouse heart after injury. (A) Flow cytometric analysis showing infiltration of CD3⁺CD4⁺hCD2⁺ Treg into the injured myocardium at day 7 post CI to the P3 heart compared to the sham control. Quantification of (B) %Treg among total CD4⁺ T-cells or (C) the absolute number of Treg per mg heart tissue within the first 2 weeks post CI based on (A). Data are presented as mean±S.E.M., n=3 per time point, *P<0.05, **P<0.01.

Figure S3

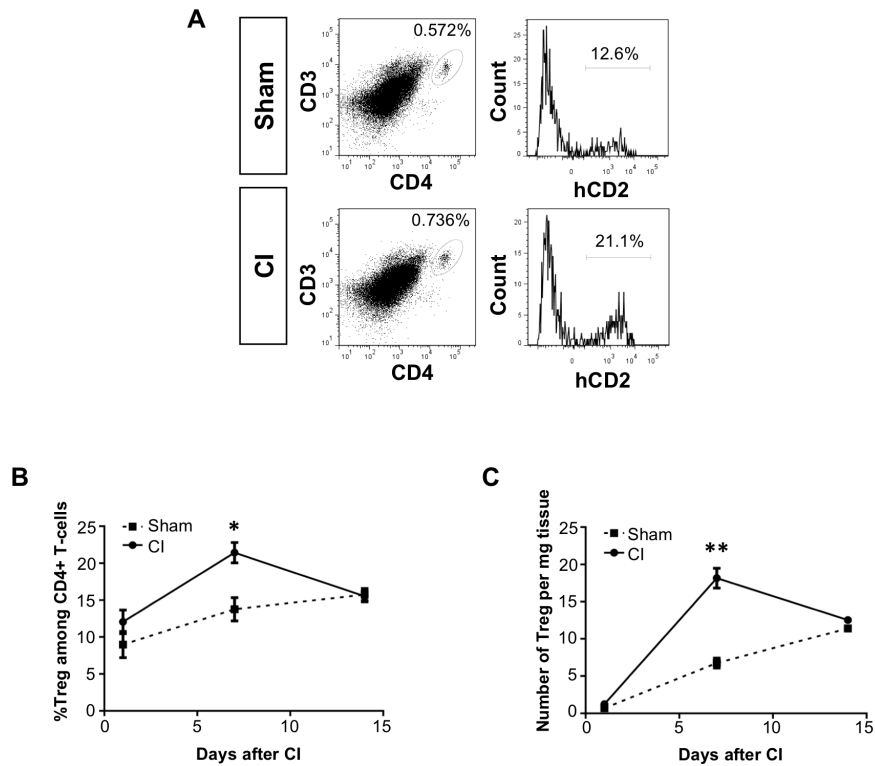


Figure S4 Depleting efficiency of PC61 targeting CD4⁺CD25^{hi}FOXP3⁺ Treg during neonatal heart regeneration. (A) Schematic diagram showing the experimental design. (B) Flow cytometric analyses and (C) quantification showing percentage of CD4⁺CD25^{hi}FOXP3⁺ Treg among total splenocytes and peripheral blood cells, respectively, at 4 weeks after CI in control or anti-CD25 (PC61) monoclonal antibody-treated groups. Data are presented as mean±S.E.M., n=8, **P<0.01.

Figure S4

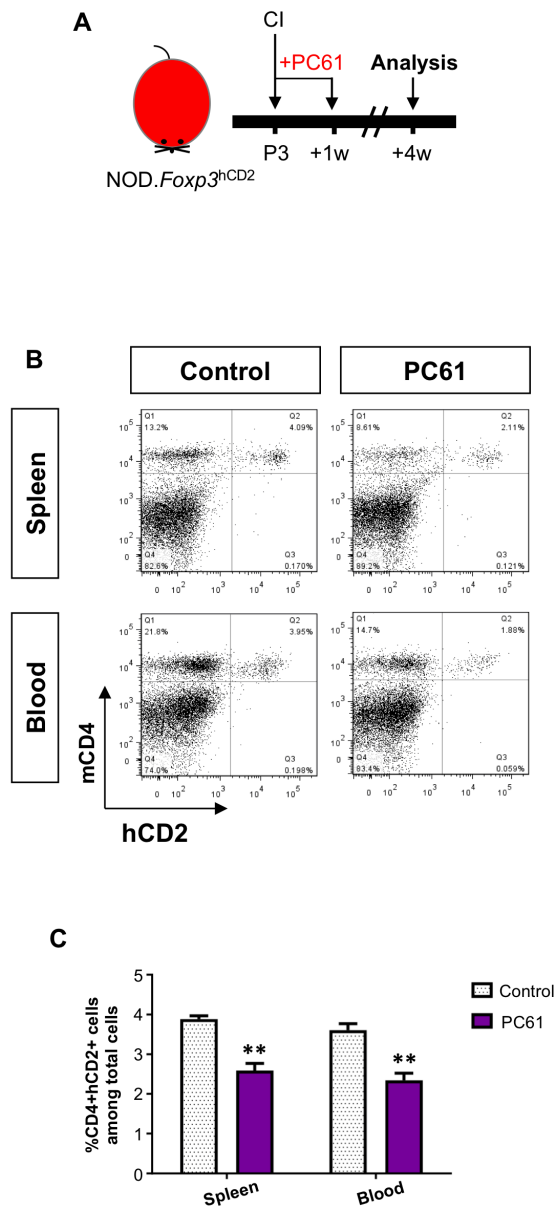


Figure S5 Loss-of-function of CD4⁺ Treg leads to increased fibrosis and reduced cardiomyocyte proliferation after cryoinfarction. (A) Images of scar tissues, scale bars: 2000 um; and Masson's trichrome staining showing representative serial cross sections of fibrotic tissues in blue, scale bars: 1000 um. (B) Quantification of fibrotic tissue coverage based on (A), n=8. Immunostaining on frozen sections for (C) COLA1⁺ (red) and cTnT⁺ (green) cells within the infarct zone or (E) Ki67⁺ (red) or pH3⁺ (red) and cTnT⁺ (green) cells within the border zone. Arrows indicate cardiomyocytes positive for Ki67 or pH3 and square denotes magnified images on the right. Quantification of (D) %cTnT⁺ coverage or the absolute number of (F) Ki67⁺cTnT⁺ or (G) pH3⁺cTnT⁺ cardiomyocytes per mm² area, n=4. (B, D, F, G) Data are presented as mean±S.E.M., *P<0.05, **P<0.01.

Figure S5

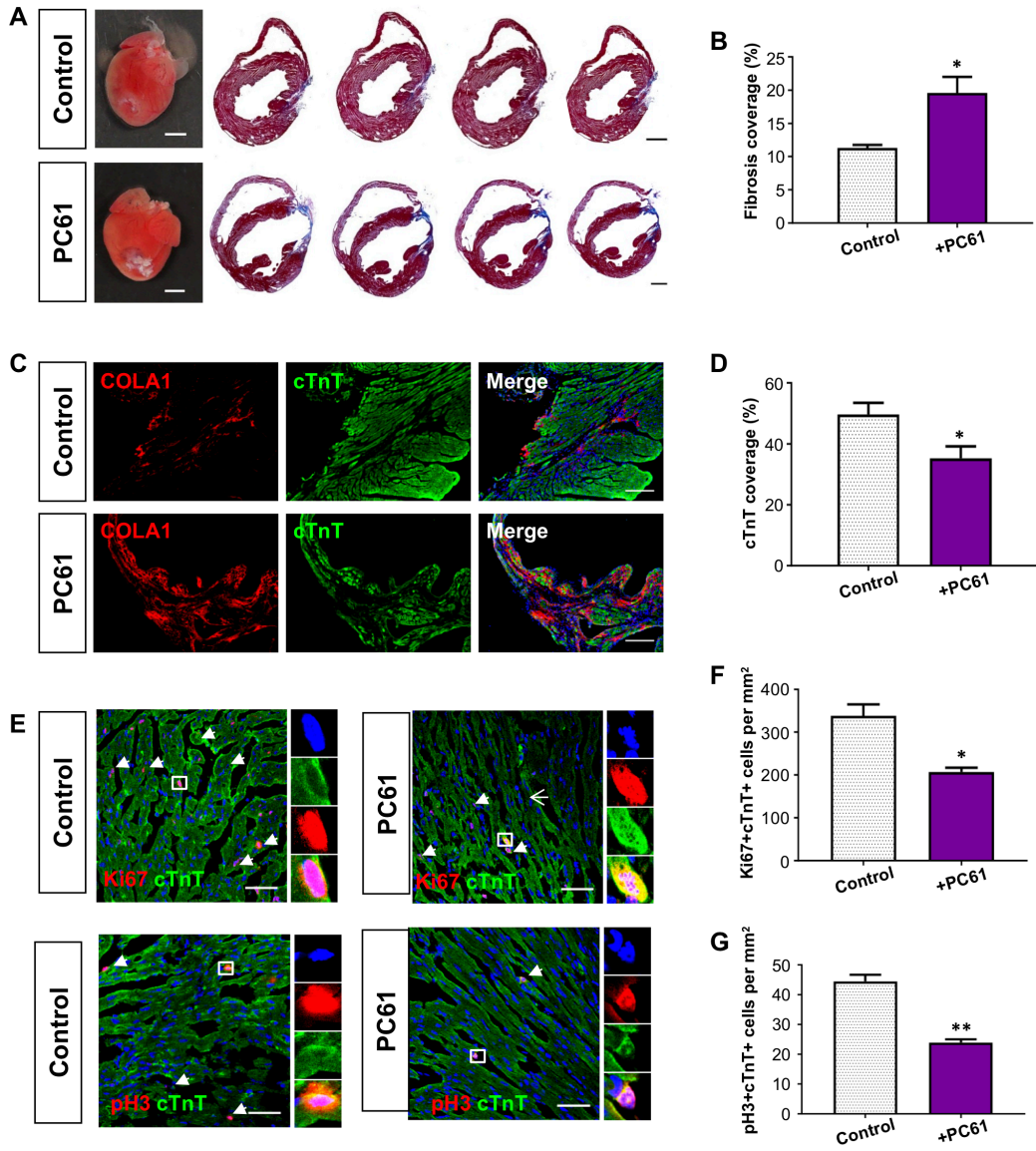


Figure S6 Cardiomyocyte characterization during neonatal heart regeneration. (A) qRT-PCR showing expression levels of the respective CDK inhibitor genes in neonatal cardiomyocytes isolated from P1 ICR mice with or without cultured in Treg SN for 1 day; gene expression levels in Treg SN were compared to control (without Treg SN). Data are presented as mean±S.E.M., n=3, *P<0.05, **P<0.01. (B) Immunostaining on frozen heart sections of the P1 heart of ICR mice for cTnT (green) and CCR3 (red). (C) Flow cytometric analysis showing expression of CCR3 on neonatal cardiomyocytes isolated from the P1 heart of ICR mice.

Figure S6

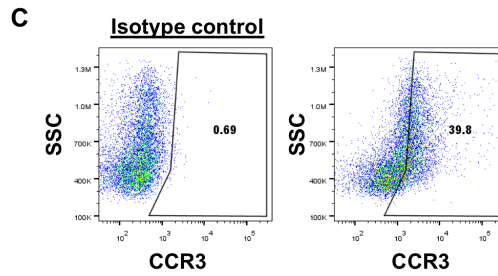
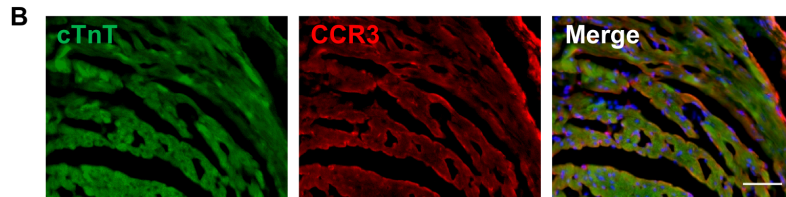
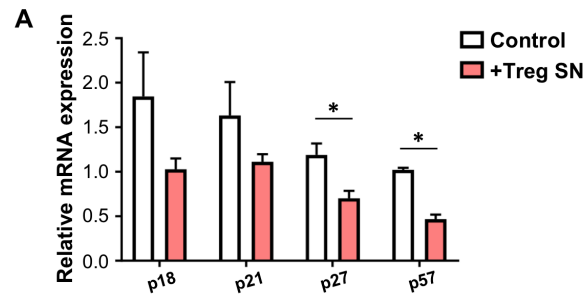


Figure S7 Treg regulate accumulation of M2-like macrophages during neonatal heart regeneration. (A, D) Schematic diagrams showing the experimental design. (B, E) Flow cytometric analysis and (C, F) quantification showing %F4/80⁺Ly6C^{high} M1-like or %F4/80⁺CD206⁺Ly6C^{low} M2-like macrophages among total F4/80⁺ macrophages after CI. Data are presented as mean±S.E.M., n=4, *P<0.05, **P<0.01.

Figure S7

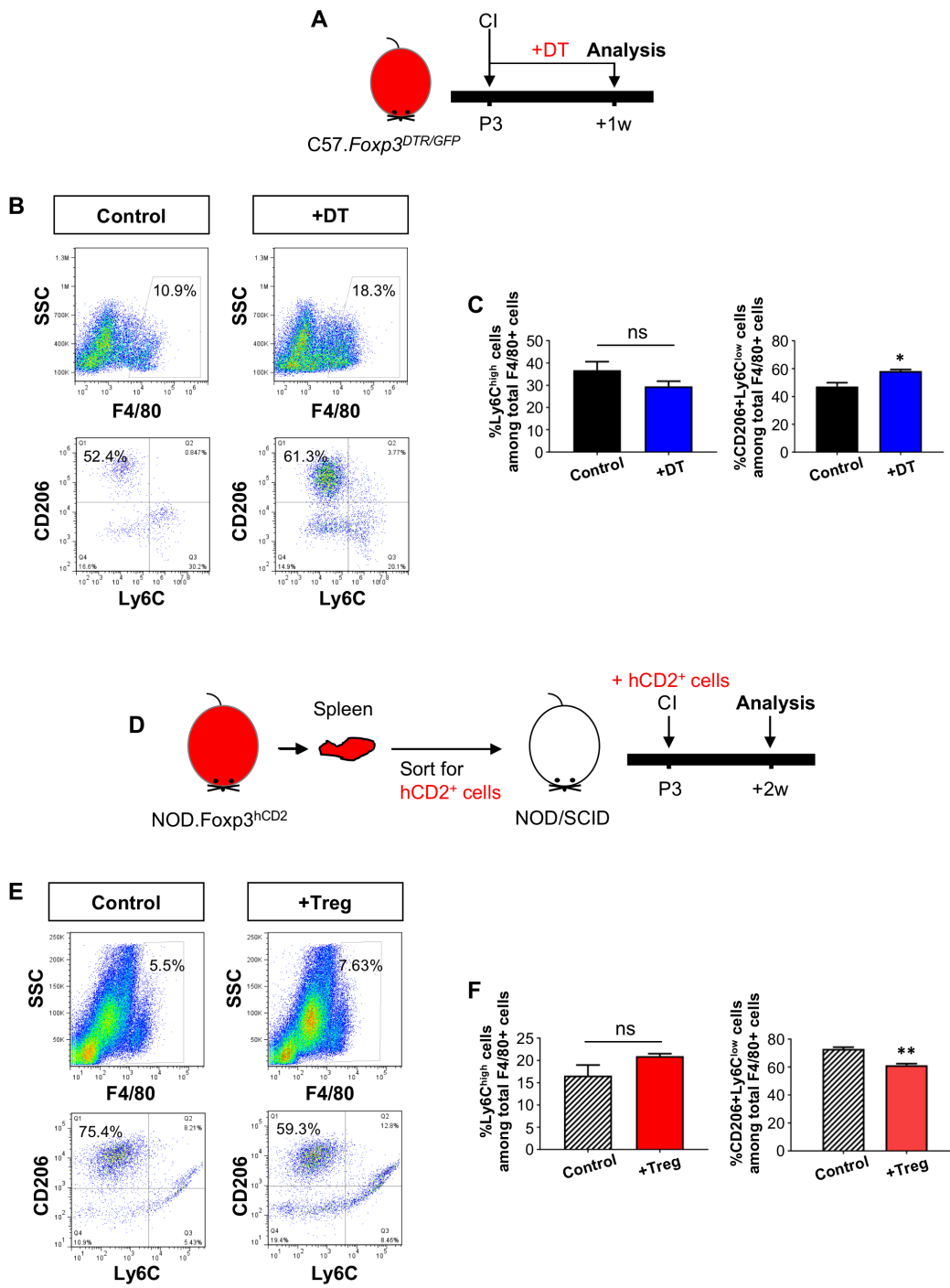


Table S1 GO functional annotations showing a list of genes expressed by C1 Treg purified from the spleen of ICR mice at day 7 after CI to a P3 heart. The selected most significantly upregulated pathways in terms of biological processes are determined by scRNA-seq.

Upregulated Pathway	p-value	Molecules
GO:0007067~mitotic nuclear division	5.78E-10	CCNB1, CDK1, CDCA8, CCNB2, NUSAP1, BIRC5, CDC20, PTTG1, UBE2C, SMC2, CDC25B
GO:0051301~cell division	1.04E-08	CCNB1, CDK1, CDCA8, CCNB2, NUSAP1, BIRC5, CDC20, PTTG1, UBE2C, SMC2, CDC25B
GO:0007049~cell cycle	1.04E-06	CCNB1, CDK1, CDCA8, CCNB2, NUSAP1, BIRC5, CDC20, PTTG1, UBE2C, SMC2, CDC25B
GO:0032496~response to lipopolysaccharide	5.86E-06	HMGB2, S100A8, WFDC21, ELANE, MPO, CD6, TNFRSF4
GO:0002376~immune system process	2.58E-05	LCN2, HMGB2, S100A8, TAP2, S100A9, FCNB, PGLYRP1, LTF

Table S2 GO functional annotations showing a list of genes expressed by C2 Treg purified from the myocardium of ICR mice at day 7 after CI to a P3 heart. The selected most significantly upregulated pathways in terms of biological processes are determined by scRNA-seq.

Upregulated Pathway	p-value	Molecules
GO:0030593~neutrophil chemotaxis	2.12E-16	CCL24, CCL12, CCL3, CCL2, C5AR1, CXCL2, FCER1G, CCL4, CCL7, FCGR3, SYK, SPP1
GO:0006935~chemotaxis	1.00E-13	CCL24, CCL12, C3AR1, CCL3, CCL2, C5AR1, CCR1, CXCL16, CXCL2, CX3CR1, CCL4, CCL7
GO:0070374~positive regulation of ERK1 and ERK2 cascade	3.93E-10	CCL24, CCL12, CCL3, CCL2, C5AR1, CCR1, TREM2, CCL4, CCL7, GAS6, CSF1R
GO:0002548~monocyte chemotaxis	1.72E-07	CCL24, CCL12, CCL3, CCL2, CCL4, CCL7
GO:0048246~macrophage chemotaxis	1.11E-05	CCL12, CCL3, CCL2, CX3CR1